Available online at www.sciencedirect.com
SCIENCE DIRECT®
Thermochimica Acta 425 (2005) 69–74
thermochimica acta
www.elsevier.com/locate/tca

Quantitative determination of heat conductivities by scanning thermal microscopy

H. Fischer*

TNO TPD Innovative Materials, P.O. Box 595, 5600 AN Eindhoven, The Netherlands
Faculty of Aerospace Engineering, TU Delft, Kluyverweg 1, 2629 HS Delft, The Netherlands

Received 13 April 2004; received in revised form 10 June 2004; accepted 13 June 2004
Available online 4 August 2004

Abstract

The possibility to use the scanning thermal microscope for a quantitative determination of the local heat conductivity λ at material surfaces is evaluated and critically discussed. Two different methods of operation have been applied: the determination of the probe to sample heat flux in the local thermal analysis (LTA) mode and the analysis of heat flow data derived from thermal maps in scanning experiments (SThM). Both methods lead to a comparable accuracy in the determination of λ. The SThM shows the highest sensitivity for small λ, and is useful in a λ range between 0.05 and 20 W/m K. Finally a new multiwire calibration standard is introduced.

Keywords: Heat conductivity; Quantitative determination; Scanning thermal microscopy; Local thermal analysis

1. Introduction

In materials design and development, there are many instances where absolute values of thermal parameters are needed. This applies to more special application areas, such as aircraft and spacecraft construction and microelectronics, as well as to many more mundane fields of construction and design in general. A quantitative determination of thermal parameters on a mesoscale would benefit especially application areas, where thermal properties at the relevant scale differ significantly from the macroscopic value, and reliability of the component depends on controlling heat/temperature management at the micron level. Also, a quantitative identification of defects on a micron and sub-micron level will be the key in achieving consistent performance. In addition, there is a lack of reliable thermal conductivity measurement techniques for thin films.

Until recently, the spatial resolution of methods for absolute thermal quantification has been limited by instrumental factors such as the spot size of the heat source, or by the wavelength of IR radiation used to determine the temperature. It is therefore essential to develop a technique that provides a sub-micron resolution, which is reliable, consistent, and easy to interpret. Several papers discuss the potential of scanning thermal microscopy (SThM) as applied by the μ-TA from TA Instruments for a quantitative determination of the absolute thermal conductivity λ with a high spatial resolution and on small samples [1–12].

In general, absolute values of thermal conductivity on nanoscale are different from the value in the bulk because phonon scattering and scattering of electrons in electron gas (in metals) have their characteristic lengths. However, for most materials the experimental length scales probed by the SThM comparable with these characteristic lengths. A validation of the experimentally determined thermal conductivities, especially for the samples with dimensions of only a few microns and with high λ-values by experiments determining values of bulk thermal conductivities is currently under way.

There are two potential ways of using thermal microscopy for the quantitative determination of thermal properties, either using the AC or the DC mode [1]. Generally, modulation (AC) techniques have clear advantages over DC methods for the determination of quantitative values since they offer in principle a better reliability and resolution as demonstrated by Fiege et al. [2]. However, as demonstrated by Buzin et al. [3], the range of frequencies available in the commercial μ-TA 2990 is not well suited for quantitative measurements of the local thermal properties of surfaces. Therefore, this

* Tel.: +31-4026-50151; fax: +31-4026-50850.
E-mail address: hfischer@tpd.tno.nl (H. Fischer).

0040-6031/$ – see front matter © 2004 Elsevier B.V. All rights reserved.
doi:10.1016/j.tca.2004.06.005

paper is concentrated on the DC operation mode of the μ-TA. Ruiz et al. [4] developed a relatively simple method for deriving thermal conductivity values from measurements of the heat flux from the probe to the sample during contact. In their method the measured heat flow is corrected for convective losses by subtracting heat current for the non-contact situation and thus representing the heat loss by convection. Plotting the corrected heat flow against λ for a range of hard materials of known conductivity gave an excellent linearity. As an approximation, the following equation has been used:

$$\frac{\Delta Q}{\Delta T} = \lambda_s \pi R \tag{1}$$

where R is the material and pressure-dependent contact radius, λ_s the thermal conductivity of the sample, ΔQ the determined heat flow corrected for the heat loss to the environment and ΔT the temperature difference between sample and probe.

Gorbunov et al. [5] verified the linear dependence of ΔQ on ΔT (for a given sample) as a function of the contact radius for a number of materials. A linear relationship between the experimental data for $\Delta Q/\Delta T$ and bulk thermal conductivity for the range from 1.0 to 320 W/m K has been found; the thermal conductivity resolution was estimated to be ca. 0.2 W/m K. The sensitivity appears large enough for quantitative measurements of local thermal conductivities in multi-component systems. Buzin et al. [3] followed a similar approach. Kuo et al. [6] used the slope of the power consumption–temperature relation obtained from local thermal analysis (LTA) experiments. Here, a linear relationship was obtained for the low thermal conductivity range. However, for samples with higher thermal conductivities an exponential calibration curve was established. Majumdar [7] also explained that the technique works well for low thermal conductivity materials but not for high thermal conductivity cases.

Meinders [8] performed experiments to determine thermal conductivity values for hard and soft substrates in scanning mode. Here, a quantitative determination of λ is obtained from the average power consumption (histograms) of a homogeneous substrate surface by means of integration over all pixels of the thermal image. Typically the histograms have Gaussian shapes, which allow the determination of an average and of a standard deviation of the thermal signal, which can be considered as a measure for the experimental uncertainty. This uncertainty decreases with decreasing thermal conductivity of the reference samples. It was seen that the sensitivity of the system drops with increasing thermal conductivity of the sample. A rather steep slope was found for thermal conductivities between 0.1 and 20 W/m K, while the curve flattens above a value of about 50–1000 W/m K.

In a later study by Gorbunov et al. [9] and Tsukruk et al. [10], Eq. (1) has been adjusted to

$$\frac{\Delta Q}{\Delta T} = \frac{3}{4}\lambda_g \pi R \tag{2}$$

where λ_g is the generalized thermal conductivity, defined as $1/\lambda_g = (1/\lambda_p) + (1/\lambda_s)$, and λ_p is the thermal conductivities of the tip of the thermal probe.

This equation can also be reformulated as

$$\frac{\Delta Q}{\Delta T} = \frac{3}{4}\frac{\lambda_p \pi R}{1 + \lambda_p/\lambda_s} \tag{3}$$

Eq. (3) demonstrates that for all surfaces with $\lambda_s \ll \lambda_p$ (polymers, glass, and semiconductors), the "composite" thermal conductivity is primarily determined by the lower conductive part, the surface. In these cases, the experimentally determined thermal conductivity is directly proportional to that of the tested material. On the other hand, for materials with a thermal conductivity higher than that of the tip material (platinum), the surface represents a thermal sink and the thermal tip becomes the poorly conductive counterpart. In that case, Eq. (3) predicts a constant generalized thermal conductivity, $\lambda_g - \lambda_p$, which is independent of the material tested. Guo et al. [11] published a similar relation.

Lefevre et al. [12] provided analytical and numerical thermal modeling (FEM) of the tip and sample, and examined the role played by the different heat exchange factors on a basic conductivity calibration. A simple expression was generated indicating that, in the present configuration of the SThM, radiative heat flux is negligible and convective heat flux represents only 4% of the input joule power. The major portion of the joule flux goes to the silver coating of the probe wire (conduction loss to the thermal element supports, ∼66%) and the sample (∼30%) and can be described by the following equation:

$$\Delta Q = \frac{A\lambda_g}{B + \lambda_g} \tag{4}$$

This equation shows that a linear dependence between Q and λ_s does not apply over the full range of λ and the sensitivity of the μ-TA appears to be limited to a certain range of thermal conductivity starting from 0.1 to a few dozen W/m K. Experiments carried out by scanning reference samples with known thermal conductivity ranging from 1.48 to 429 W/m K have verified this relationship.

This paper deals with experiments to enable a quantitative determination of heat conductivities of materials ranging from 0.1 to 600 W/m K using the μ-TA in two different operation modes (LTA and SThM). Furthermore, a new multiwire calibration standard for thermal conductivities in the range between 0.05 and 20 W/m K is introduced.

2. Experimental

Experiments to determine master curves for thermal conductivity determination were performed on a series of reference materials of known thermal conductivities; the values with references are indicated in Table 1. The roughness (RMS) of the calibration samples was between 40 and 60 nm as determined using an AFM probe in contact mode. Sets of

Table 1
Bulk materials used for the thermal calibration curve at room temperature (20 °C)

Bulk material	λ (W/m K)
Air	0.024
Promat thermal insulation material	0.024
PP	0.17
PS	0.14
PMMA	0.19
PC	0.18
PET	0.27
HDPE	0.37
Epoxy	**0.18**
PZT	1.5
Glass	**1.6**
ZrO_2	1.6
SiO_2	2
Steatit	2.5
Ti	17
Al_2O_3	**30**
Pb	33
Ta	54
Ni	60
Sn	63
Pt	**69**
Brass	113.5
Si	124
SiC	125
Mo	138
W	164
Graphite	200
Al	205
Au	**405**
Cu	**330**
BN	360

thermal data (slope of the power consumption–temperature relation obtained from local thermal analysis, LTA) were collected at four different locations on a 100 μm × 100 μm scan for three different scan areas for each sample with a heating speed of 5 K/s between 25 and 100 °C (see Fig. 1). Additionally the thermal maps (histograms of the power signal derived from the spatial pixel values in the thermal image) were collected for each sample at the three areas using a scanning speed of 3 Hz and a contact pressure of app. 5 kPa [13]. For all samples, thermal measurements were repeated with two different tips and gave consistent results (<20% differences). In all scanning experiments, the temperature of the tip was set to 80 °C after a proper calibration of the temperature–resistance relation following known procedures. Although the thermal conductivity of most materials is temperature-dependent, reference values for temperatures of ca. 25–30 °C were used since the surface temperature of the substrate was in most of the cases much lower than the tip temperature [12]. The surface temperature dropped even to below 30 °C for the well-conducting samples such as aluminum. It is therefore not expected that the measured value deviate significantly from the values at room temperature. This statement was supported by the measurements of the sample heat flow as a function of the tip temperature for several sample materials, the linearity of these curves indicated that the thermal conductivity of the sample was at least not strongly temperature-dependent in the temperature range in which the measurements were performed [8]. The set temperature of 80 °C was selected to obtain sufficient thermal contrast. The influence of the surface roughness onto the quantitative detection of heat conductivities has been explored while scanning glass samples with different roughness (RMS) values ranging between 10 nm and ca. 8 μm using a probe temperature of 200 °C.

The calibration of the relation between the determined heat flow and λ is tedious and time-consuming, substantial wear of the probe wire will occur and each time a new probe has to be used. Therefore, a new calibration standard has been designed (see Fig. 2). This calibration standard consists of fine wires of Au, Cu, and Pt as well as fibers of SiO_2 and Al_2O_3, all with diameters between 5 and 30 μm spanning over a range of thermal conductivities (Table 1, bold letters) embedded in an area of 100 μm × 100 μm, which is the maximal scanning range, in epoxy resin and polished to a RMS ∼10 nm. The wire material was chosen to display a range of λ values coupled with chemical and especially oxidative stability, and durability, combined on a small surface and thus enabling a calibration over a considerable range of λ-values in one shot. Alternatively, it is now possible to get a λ calibration for different scanning temperatures for one and the same probe. A more specific calibration in a λ

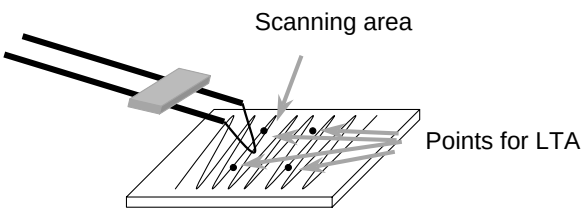

Fig. 1. Scheme of the experiments performed for the determination of λ.

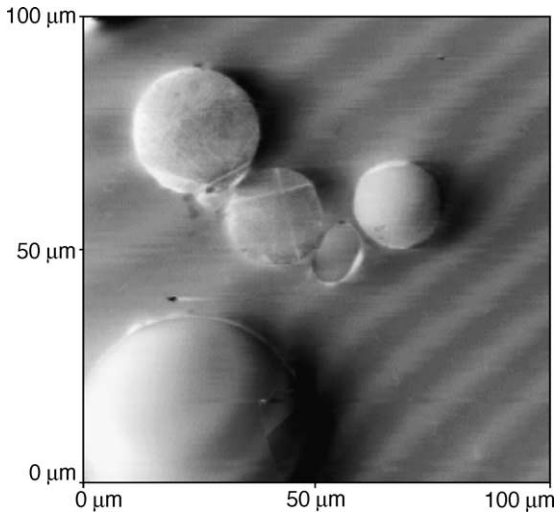

Fig. 2. Plot of a surface scan of the polished calibration standard.

range of choice is also possible if the choice of wires will be adjusted to the needed range. Again, maxima of the histograms of the spatial pixel values in the thermal image, in this case of selected areas, for obtaining an averaged heat of the different materials combined in the standard are used. The scanning temperature was also 80 °C.

3. Results and discussion

A quantitative determination of heat conductivities via the μ-TA is possible using two different methods of operation (LTA and SThM) parallel to each other. The relation between λ and $\Delta Q/\Delta T$ as derived from LTA experiments for standard samples with known heat conductivities (Table 1) is plotted in Fig. 3a. Fig. 3b shows a plot of data obtained from SThM experiments. The heat flow was corrected for heat losses to the environment via subtraction of the baseline heat losses, measured in air. A fit using Eq. (4) through both data sets gives master curves for the two methods. As to be seen, the fit is satisfactory, the fit parameters for both methods are listed in Table 2. The master curve may now be used to derive the effective thermal conductivity of unknown samples via a comparative evaluation of the measured heat flow under identical experimental conditions (contact force, roughness, ambient temperature, tip temperature, etc.). Clearly the most sensitive area of λ to be measured with this instrument ranges between 0.05 and 20 W/m K. The instrument appears to be most sensitive for samples with low λ-values, with small differences of λ in the lower λ-range providing an optimum of the tip-sample conductance which is temperature- and topography-dependent, very much in accordance to the theoretical predictions by Lefevre et al. [12].

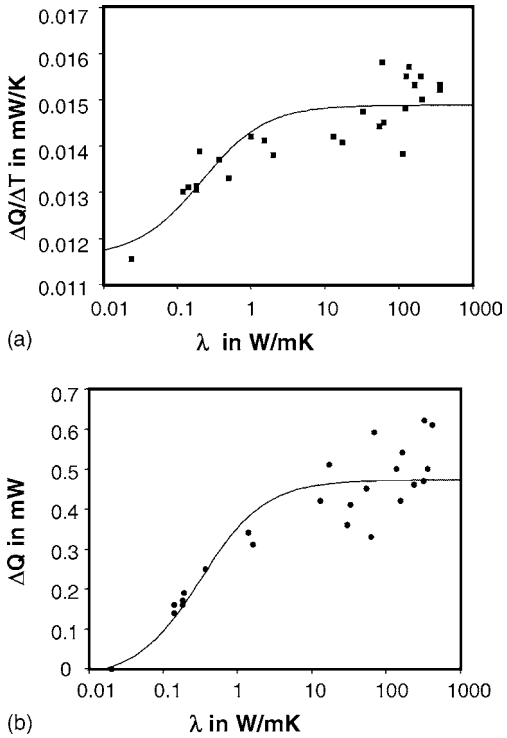

Fig. 3. (a) Plot of the slope of the power consumption–temperature relation data as obtained from local thermal analysis (LTA; $\Delta Q/\Delta T$) vs. the thermal conductivity of several test samples. The slope was taken for temperatures between 50 and 80 °C. The line is the best-fit according to Eq. (4). (b) Plot of the averaged heat flow, corrected for losses to the environment by subtraction of the baseline signal, vs. the thermal conductivity of several test samples. The temperature of the tip was T = 80 °C. The line is the best-fit according to Eq. (4).

Table 2
Fit parameters of the master curves in Fig. 1 according to Eq. (4)

Method	Slope ($\Delta Q/\Delta T$)	Heat flow (ΔQ)
A (W)	0.011	0.025
B (W/m K)	0.038	0.32
R-value	0.91	0.93

Other reasons for a large error ranges for samples with high λ will arise due to differences in roughness of the samples onto the detection of quantitative values and uncertainty in the λ values of the samples used.

The contact radius d under elastic deformation conditions can be calculated as follows:

$$d = \left(\frac{6FR_{\text{tip}}}{E^*}\right)^{1/3} \tag{5}$$

with R_{tip} representing the radius of the loop of the tip wire, F equals the contact force and E equals the effective elastic modulus, which is

$$E^* = \left(\frac{1-\nu_1^2}{E_1} + \frac{1-\nu_2^2}{E_2}\right)^{-1} \tag{6}$$

and ν_1 and ν_2 being Poisson's ratio the tip and the surface material, respectively.

Under the current experimental conditions, the thermal contact diameter is determined to be about 30 nm for hard materials [5]. This value correlates with an estimate for the thermal resolution limit made from thermal images for silicon oxide–silicon grids (<0.1 μm). Such an extremely low effective thermal contact area can be related to asperity-assisted effective sharpening of the thermal probe as was observed for graphite samples, where a lateral thermal resolution of about 50 nm was detected. However, direct estimates of the thermal contact size in soft (polymeric) materials gives values closer to 1 μm. Obviously, in this case, the effective thermal contact area is determined by the area of direct mechanical contact that is much larger for compliant materials with a low elastic modulus.

In case the surface roughness exceeds the contact radius a dramatic influence onto the accuracy of determination of heat flow to the sample is expected mainly due to local changes of the effective contact area. This has been demonstrated while scanning samples of the same material (glass, λ = 1.6 W/m K) with different roughness values. The result of this set of experiments is depicted in Fig. 4. Here, the maxima of the histograms of the spatial pixel values in the

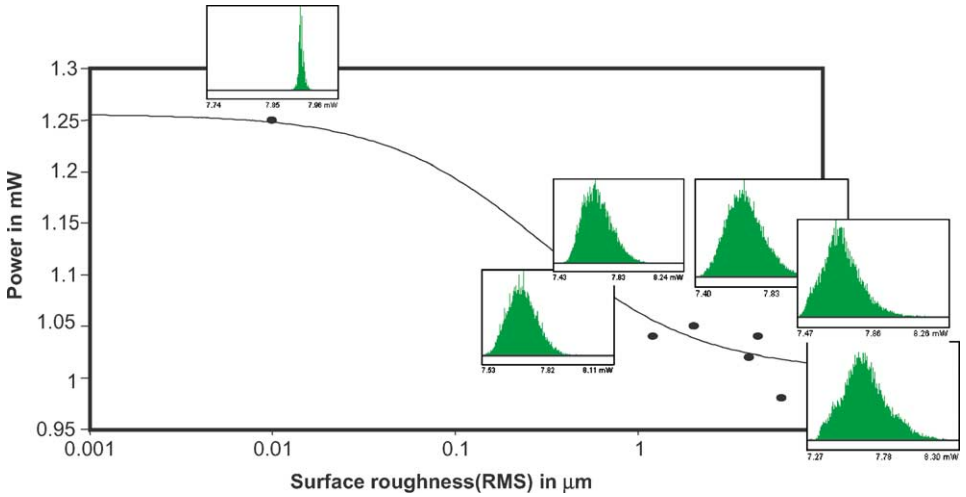

Fig. 4. Plot of the averaged power signal (power consumption) obtained during scanning glass surface with different roughness at 200 °C vs. the determined surface roughness. The line is the best-fit according to Eq. (7); the insets show the spatial distribution of pixel values in the thermal images of the individual samples.

thermal image for obtaining an averaged heat flow have been plotted against the surface roughness (RMS value) of the samples under investigation. Additionally, the histograms of the spatial pixel vales are placed within the graph. It is immediately clear that only a very smooth surface with a good defined contact area leads to quantitative and reproducible values of λ. When the RMS reaches values of more than 1 μm, heat flow (power) versus surface roughness levels off. This can easily be explained if one considers the size of the probe wire. When the surface roughness scales in the same order as the diameter of the wire, a situation is reached where complete contact may be not realized at all locations. This broadens the distribution of the spatial pixel values in the thermal images. At very high roughness values (RMS >5 μm), the probe will even be able to penetrate into holes increasing the contact area dramatically. This again can be followed with the spatial pixel values in the thermal images; in this range a bimodal distribution becomes visible.

The function of the determined heat flow follows the empirical equation:

$$\Delta Q = \Delta Q_0 - \frac{Ax}{B + x} \tag{7}$$

whereby ΔQ_0 denotes the heat flow for an ideal smooth surface, x denotes the surface roughness, A and B are adjustable parameters. It can be clearly seen that starting with an average surface roughness of ca. 40 nm the tip starts loosing complete contact with the surface resulting in a smaller heat flow towards the sample. Therefore, a quantitative determination of heat conductivities of unknown samples requires besides a good calibration of the probe also a sufficiently smooth surface. This is especially true for samples with a low λ. Samples with a high λ may tolerate a higher surface roughness for a reliable determination of λ since the thermal contact is larger than the mechanical one due to side micro-heat exchange.

Fig. 5 shows the spectrum of the spatial pixel values in the thermal image together with the thermal image of the calibration sample itself. An identification of the individual contributions of the different materials is easily possible. Also separate line scans through the thermal image, as

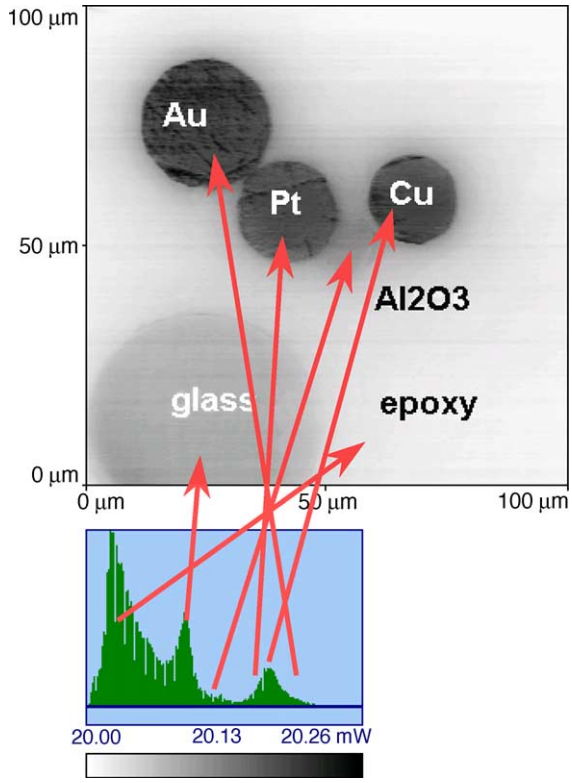

Fig. 5. Thermal image obtained from the calibration standard while scanning at 80 °C together with a plot of the spectrum of the spatial pixel values in the thermal image. An identification of the individual contributions of the different materials is easily possible and is indicated by the arrows.

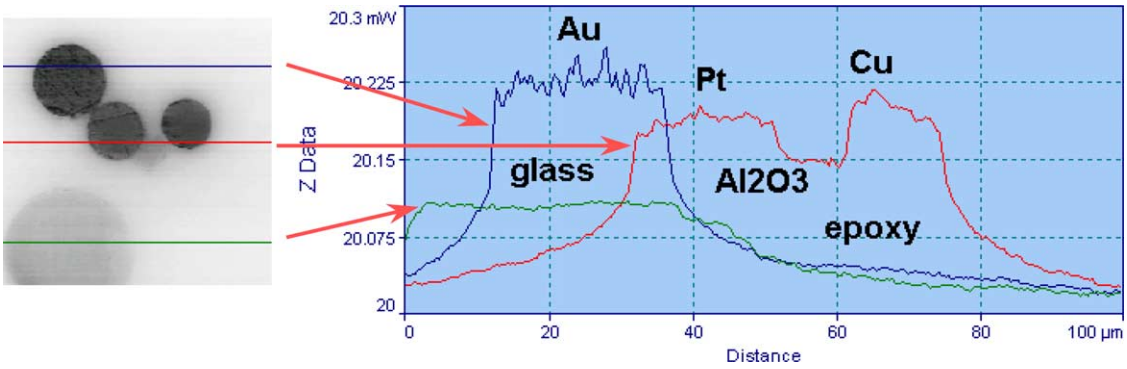

Fig. 6. Thermal image obtained from the calibration standard while scanning at 80 °C together with separate line scans through the thermal image showing the differences in heat flow to the individual materials. The heat flow from the probe to the sample is higher for materials with larger λ.

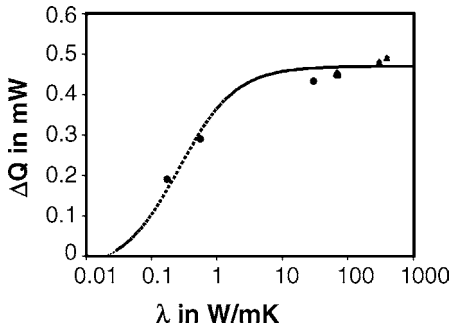

Fig. 7. Plot of the averaged heat flow, corrected for losses to the environment by subtraction of the baseline signal, vs. the thermal conductivity of the individual several test samples. The temperature of the tip was $T = 80\,^{\circ}C$. The line is fit displayed in Fig. 3b.

depicted in Fig. 6, show clearly the differences in heat flow to the individual materials. The heat flow from the probe to the sample is higher for materials with larger λ as expected.

Finally the quantitative heat flows are plotted in Fig. 7. Additionally, the fit function as obtained from the calibration samples (Fig. 3b) is shown. The data points obtained from the calibration standard fit very well to the function elucidated; hence the standard can be used for a quick and reliable calibration of thermal probes for a quantitative determination of λ of unknown samples with an accuracy of ±10%. The wear of the probe while scanning the standard is negligible, one and the same probe can be used many times.

4. Summary

The possibility to use the scanning thermal microscope for a quantitative determination of heat conductivities of surfaces of materials is evaluated and critically discussed. Two different methods of operation have been applied, the determination of the heat flux from the probe to the sample during contact in the LTA and the analysis of heat flow data (ΔQ) derived from thermal maps from scanning experiments. Both methods lead to a comparable relation for a reliable determination of λ. The SThM shows highest sensitivity for small λ, it is useful in a λ-range between 0.05 and 20 W/m K. Also, the determination of quantitative data of λ is highly sensitivity to the surface roughness of the sample. The surface roughness should be below 30 nm (RMS value) to guarantee a correct determination of the heat conductivity. Finally a new calibration standard is introduced proving a possibility of a quick and easy calibration of thermal probes with respect to λ.

Acknowledgements

The supply of the thin metal wires used for the new calibration standard by A. Schneidewind, Department für Geo- und Umweltwissenschaften, LMU München is gratefully acknowledged.

References

[1] H.M. Pollock, A. Hammiche, J. Phys. D: Appl. Phys. 34 (2001) R23–R53.
[2] G.B.M. Fiege, A. Altes, R. Heiderhoff, L.J. Balk, J. Phys. D: Appl. Phys. 32 (1999) L13.
[3] A.I. Buzin, P. Kamasa, M. Pyda, B. Wunderlich, Thermochim. Acta 381 (2002) 9.
[4] F. Ruiz, W.D. Sun, F.H. Pollak, C. Venkatraman, Appl. Phys. Lett. 73 (1998) 1802.
[5] V.V. Gorbunov, N. Fuchigami, J.L. Hazel, V.V. Tsukruk, Langmuir 15 (1999) 8340.
[6] C. Kuo, C.-C. Chen, W. Bannister, Thermochim. Acta 403 (2003) 115–127.
[7] A. Majumdar, Annu. Rev. Mater. Sci. 29 (1999) 505.
[8] E. Meinders, J. Mater. Res. 16 (2001) 2530.
[9] V.V. Gorbunov, N. Fuchigami, V.V. Tsukruk, Probe Micros. 2 (2000) 53, 65.
[10] V.V. Tsukruk, V.V. Gorbunov, N. Fuchigami, Thermochim. Acta 395 (2003) 151–158.
[11] F.A. Guo, K.Y. Zhu, N. Trannoy, J. Lu, Thermochim. Acta 419 (2004) 239.
[12] S. Lefevre, S. Volz, J.-B. Saulnier, C. Fuentes, N. Trannoy, Rev. Sci. Instrum. 74 (2003) 2418.
[13] H. Fischer, Macromolecules 35 (2002) 3592.